We are IntechOpen,
the world's leading publisher of
Open Access books
Built by scientists, for scientists

6,900
Open access books available

186,000
International authors and editors

200M
Downloads

Our authors are among the

154
Countries delivered to

TOP 1%
most cited scientists

12.2%
Contributors from top 500 universities

CLARIVATE ANALYTICS
BOOK CITATION INDEX
INDEXED

WEB OF SCIENCE™

Selection of our books indexed in the Book Citation Index
in Web of Science™ Core Collection (BKCI)

Interested in publishing with us?
Contact book.department@intechopen.com

Numbers displayed above are based on latest data collected.
For more information visit www.intechopen.com

Advanced MR Imaging Techniques in the Diagnosis of Intra-axial Brain Tumors

Anastasia Zikou, George Alexiou and
Maria Argyropoulou

Additional information is available at the end of the chapter

Abstract

Intracranial masses are a significant health problem and present several imaging challenges. The role of imaging is no longer limited to merely providing anatomic details but the advanced MR techniques permit the assessment of the freedom of water molecule movement, the microvascular structure and hemodynamic characteristics, and the chemical makeup of certain metabolites of lesions. In the current chapter, we will discuss the role of the advanced MR imaging techniques, namely perfusion, diffusion-weighted imaging, and MR spectroscopy in the diagnosis and classification of the most frequent brain tumors in adults. We provide a brief description of the advanced MR techniques that are currently used, and we discuss in detail the imaging findings for each lesion. These lesions include gliomas both high and low grade, metastatic lesions, lymphomas, and lesions that may mimic tumors such as tumefactive demyelinating lesions, abscesses, and encephalitis. Our goal is to summarize the diagnostic information that advanced MR imaging techniques offer for establishing a diagnosis and clinical decision making.

Keywords: MRI, brain tumors, perfusion, diffusion tensor imaging, spectroscopy

1. Introduction

Among primary brain and central nervous system tumors in adults, meningiomas are the most common, accounting for 36.4% of all, followed by pituitary tumors (15.5%) and glioblastoma (WHO Grade IV) (15.1%), which is the most malignant primary brain tumor. Other types are nerve sheath tumors (8.1%), all other astrocytomas (5.7%), lymphoma (2%), ependymal tumors

(1.9%), oligodendrogliomas (1.6%), embryonal tumors (1.1%), oligoastrocytic tumors (0.9%), and all other less frequent tumors (11.7%) [1].

Imaging has a fundamental role in intracranial tumor management. Magnetic resonance imaging (MRI) is the imaging modality of choice for establishing diagnosis, classification, surgical planning, and post-treatment follow-up. The latest MRI techniques, namely diffusion, perfusion, and spectroscopy, offer more than the anatomical information that conventional imaging provides. Diffusion allows the assessment of water displacement within tissue. Diffusion tensor imaging permits the mapping of axonal organization. Perfusion MRI is a technique for the assessment of cerebral perfusion. Dynamic susceptibility contrast imaging (DSC-MRI) perfusion technique is currently the most widely used and allows the calculation of relative cerebral blood volume (rCBV) and relative cerebral blood flow (rCBF). MR spectroscopy, with single-voxel or multi-voxel techniques, can detect metabolites within tissue such as N-acetyl aspartate (NAA), choline-containing compounds (Cho), myoinositol (mI), lactate (Lac), creatine (Cr), and other molecules. However, no tumor-specific metabolite has been recognized to date.

Although the discrimination between intra-axial and extra-axial lesions is relatively straightforward, for the accurate discrimination of the variety of intra-axial tumors of several difficulties exist. This is of paramount importance for timely and appropriate patients' management. Herewith, we provide an overview of the latest MR techniques for the differential diagnosis of intra-axial tumors.

2. Primary tumors

Gliomas are the most common primary brain tumors. Glioblastoma accounts for 55% of all cases followed by diffuse astrocytoma (8.6%), ependymal tumors (6.9%), anaplastic astrocytomas (6.1%), oligodenrogliomas (5.7%), pilocytic astrocytomas (5.2%), and other less frequent glioma types [1]. Incidence is higher in males and in whites than in blacks. For glioblastoma, the median age of diagnosis is 64 years but for low-grade gliomas (grades I and II), most often occur between 20 and 40 years. The major diagnostic goal in gliomas is the differentiation of low-grade from high-grade gliomas and from other pathologies that have similar imaging features.

2.1. Diffusion-weighted imaging

Apparent diffusion coefficient (ADC) maps alone cannot differentiate between glioma from another neoplasm or glioma type. Malignancy is usually associated with increased cellular density, resulting in decreased signal intensity on ADC images. High-grade gliomas usually have significant lower ADC values than low-grade gliomas. A lesion-to-normal (L/N) ADC ratio of 1.43 could differentiate low-grade from high-grade gliomas with 100% sensitivity and 94.4% specificity [2]. Evaluation of the perilesion area may aid the diagnosis of a primary tumor due to its infiltrative nature (**Figure 1**).
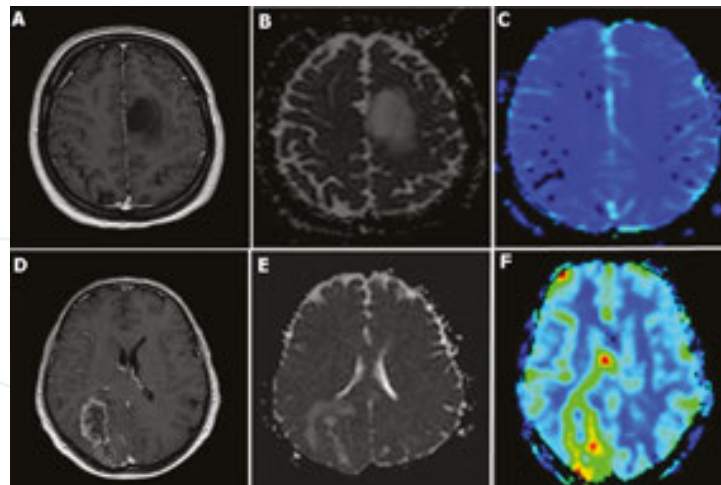
Figure 1. (A) A case of a grade II astrocytoma and of glioblastoma (D). There is a lower ADC value in astrocytoma (B) than glioblastoma (E). The rCBV map shows increased perfusion in glioblastoma (F) contrary to astrocytoma (C).

2.2. Perfusion imaging

Perfusion MRI can be performed using a variety of methods. The most common techniques are as follows: T2-weighted dynamic susceptibility contrast (DSC), T1-weighted dynamic contrast enhanced (DCE), and arterial spine labeling (ASL). The latter do not require contrast administration. The relative cerebral blood volume (rCBV) is the most frequent reported metric. This can be calculated by comparing the cerebral blood volume in a region of interest that is drawn over the tumor to the CBV of a mirror region of interest placed over the normal white matter in the contralateral side.

Gliomas are characterized by increased blood vessels formation for the transport of nutrients and oxygen which are essential for tumor growth. Furthermore, apart from glioma infiltration to parenchyma, malignant cells can also migrate using a perivascular route through microvasculature [3]. Recent reports showed that glioblastoma cells can even differentiate into endothelial cells and pericytes, thus aiding tumor vascularization [4]. High-grade gliomas have a significantly higher rCBV ratio than low-grade gliomas (**Figure 1**). A cut-off ratio of 0.63 has been suggested for the differentiation between them [2]. Furthermore, a significant linear correlation has been reported between rCBV ratio and glioma proliferation potentials as assessed by Ki-67 index and tumor's cell cycle analysis [5, 6]. High-grade tumors had higher Ki-67 index, higher percentage of cells in G2/M phase, and lower percentage of cells in G0/G1 phase.

Oligodendrogliomas contrary to other low-grade gliomas have significant higher rCBV values (mean 3.68 ± 2.39) [7], overlapping even with high-grade gliomas. A possible explanation to this is their increased vascular density and cortical localization [7]. Another important exception is pilocytic astrocytoma, the most common pediatric brain tumor with usually infratentorial localization [8]. The tumor's mural nodule may show increased rCBV ratio in comparison with other low-grade gliomas. Clinicians should also bear in mind that hemangioblastomas may also demonstrate high rCBV ratios.

2.3. MR spectroscopy

Initial studies with MR spectroscopy showed promise for the diagnosis of brain lesions and grading; however, recent evidences are controversial. Several metabolites can be measured that correlate with various pathological alterations within lesions. NAA is the acetylated form of the amino acid, aspartate, which is found in increased concentrations in viable neurons. Given that non-neuronal neoplasms destroy normal neurons there is a reduction in NAA signal. Choline is a marker of cell membrane and can be found elevated in tumors and inflammatory processes. Creatine is a measure of energy stores, whereas lactate increases in cases of ischemia, in which the cell switches to anaerobic glycolysis and lactates accumulates. Thus, lactate is more likely to be present in high-grade than low-grade gliomas. Lipids have been recognized as a marker of myelin breakdown. Several studies have evaluated both single-voxel and multi-voxel spectroscopy. Multi-voxel has the advantage of greater spatial resolution and extent of coverage, thus permits the evaluation of different components of heterogeneous masses. Within tumor, some areas may be more metabolically active than others. In brain tumors, there is usually an increased signal of Cho, whereas NAA and Cr are reduced. Cho/Cr ratio tends to increase as glioma malignancy progresses. In a recent meta-analysis, Cho/NAA ratio showed a sensitivity of 80% and specificity of 76%, higher than Cho/Cr ratio and NAA/Cr ratio for the differentiation of high-grade from low-grade gliomas [9]. However, both sensitivity and specificity do not enable an accurate diagnosis, thus additional imaging modalities may be needed. A CHO/NAA ratio >1, in voxels outside of the enhancement region, suggests tumor infiltration and is indicative of a high-grade glioma (**Figure 2**).
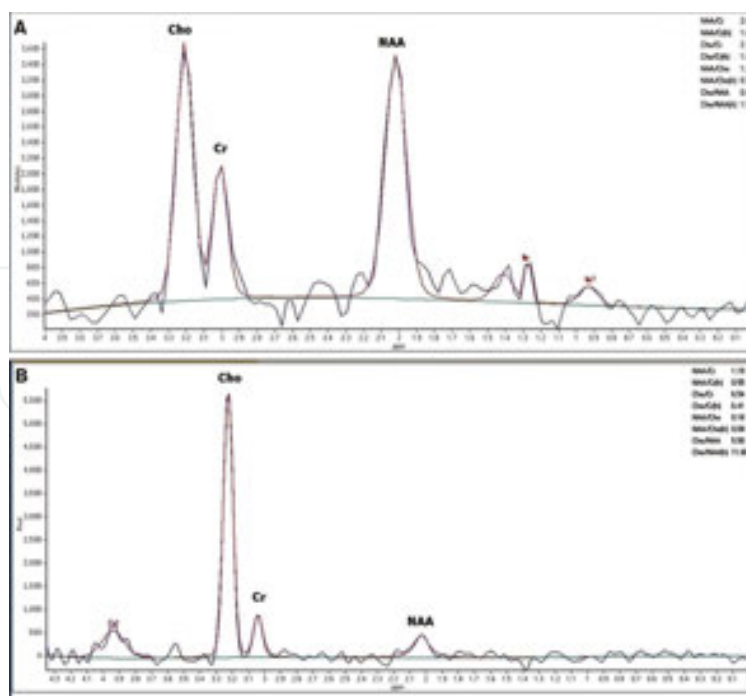

Figure 2. MR proton spectrum of a grade II astrocytoma (A) and of a glioblastoma (B). Contrary to low-grade glioma, glioblastoma exhibits depression of the NAA and creatine (Cr) peaks and elevation of the choline (Cho) peak.

3. Gliomatosis cerebri

Gliomatosis cerebri is a rare diffuse primary neoplastic process of glial origin with dismal prognosis. Based on WHO criteria, this diffusely infiltrating glial neoplasm involves at least three cerebral lobes. There is often bilateral involvement of the cerebral hemispheres and/or deep gray matter (**Figure 3**) [10]. Histopathologically, it is characterized by diffuse infiltration of brain parenchyma by small, immature glial cells that resembles astrocytes, oligodendroglia, or undifferentiated cells [10, 11]. The lesion can contain areas of WHO grades II or III tumors, and less frequent grade IV. Symptomatology is subtle and may involve changes in personality and mental status, headache, hemiparesis, ataxia, and seizures. Although it appears radiologically as extensive disease, clinical symptomatology may be silent. Diagnosis requires brain biopsy and histopathological examination.

Figure 3. T2-W axial images show diffuse hyperintense lesions with enlargement of the involved structures and little mass effect (arrows).

Two subtypes can be identified radiologically: type 1 with no discrete component and type II with a solid component and diffuse CNS involvement. *IDH1* mutations have been reported more frequent in type II GC [12]. MRI findings are essential for establishing the correct diagnosis. Hypointensity in T1-weighted sequences and hyperintensity in T2-weighted and FLAIR sequences are the classical findings. Another usual MRI finding consists of diffuse infiltration of the cortex with an enlargement of the cortical sulci and the absence of clear

delineation between white and gray. Contrast enhancement is absent [13]. In DWI, there is usually no restriction. Perfusion MR shows low or normal rCBV values correlating with the absence of vascular hyperplasia. MR spectroscopy reveals elevated Cho/NAA ratios and marked elevation of myoinositol [14] (**Figure 4**).
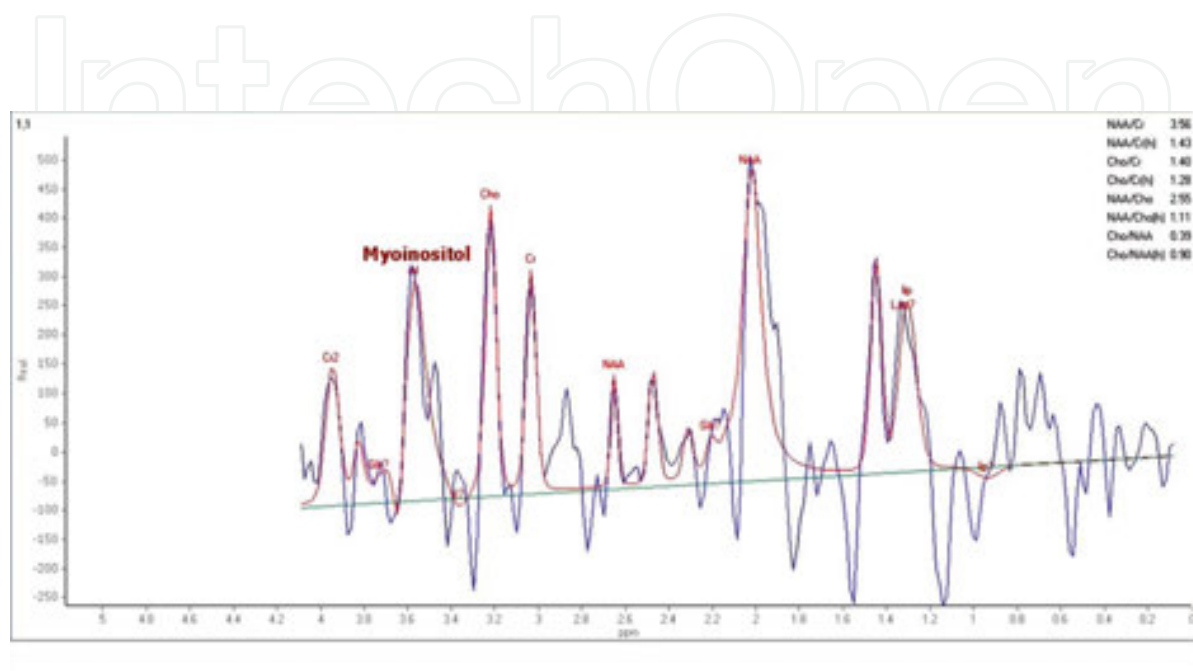

Figure 4. Short-echo MR proton spectrum shows an elevated myoinositol (mI) peak (at 3.55 ppm) in a case of gliomatosis cerebri.

4. Primary central nervous system lymphoma

Primary central nervous system lymphoma (PCNSL) is a rare variant of extranodal non-Hodgkin lymphoma and affects about 1,000 people in the United States each year. Non-invasive diagnosis of PCNSL is of paramount importance given the dramatic benefits of chemotherapy in this tumor. Typical MR imaging features of PCNSLs are frequent periventricular locations, perilesional edema, well-defined margin, and homogeneous and intense nodular enhancement.

4.1. Diffusion-weighted imaging

PCNSLs tend to have a low ADC value because of high cellularity (**Figure 5**). Brain abscess has higher ADC values than lymphomas; thus, this feature can help in differentiating these two entities [15].
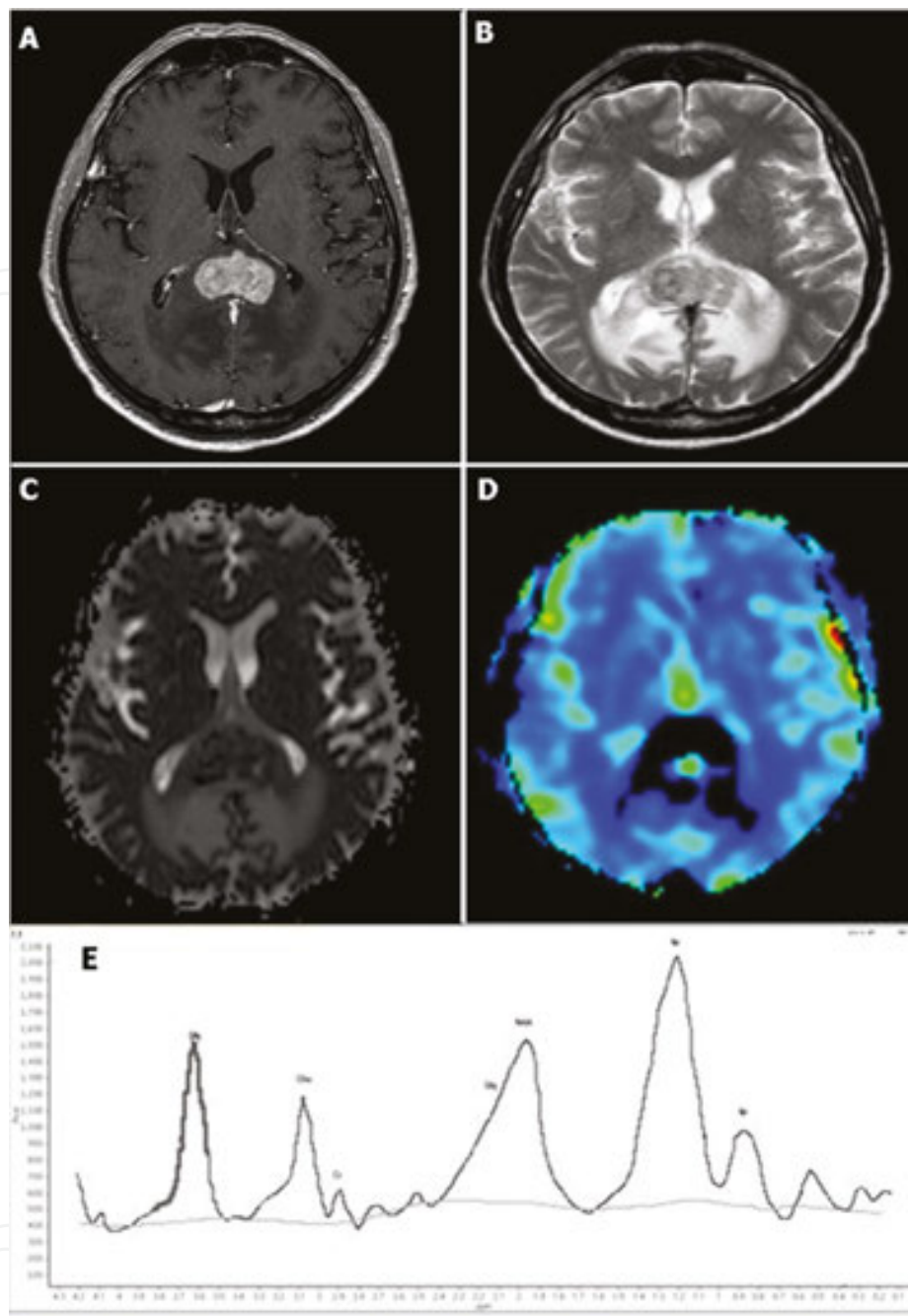
Figure 5. A case of lymphoma (A, B) revealing a low ADC value (C), low perfusion (D), and elevated levels of Lipids (E).

4.2. Perfusion imaging

PCNSL has low rCBV compared with that of high-grade gliomas and metastasis; however, overlapping values may exist (**Figure 5**). An important clue is that PCNSL demonstrates a significant increase in signal intensity above the baseline due to massive leakage of contrast media into the interstitial space contrary to high-grade gliomas [16]. Lymphoma tends to demonstrate higher rCBV compared with toxoplasmosis [15].

4.3. MR spectroscopy

Characteristic spectroscopic findings for PCNSL include elevated signals of lipid, choline, and lactate and reduced NAA signal (**Figure 5**). Large lipid peaks on lesions without central necrosis are also strongly suggestive of PCNSL [17]. High lipid peak may be due to increased turnover of the membrane components in transformed lymphoid cells.

5. Differential diagnosis

5.1. Tumefactive demyelinating lesions

Tumefactive demyelinating lesions (TDLs) can be seen either during a relapse of a known multiple sclerosis or on acute onset. TDL can mimic high-grade gliomas on conventional MRI. In both conditions, there is contrast enhancement, perilesional edema, and central necrosis. Additional histopathology is not always straightforward since abnormal mitotic figures in reactive astrocytes can be present. In TDL, there is usually incomplete rim enhancement on MRI and little mass effect and edema (**Figure 6**).
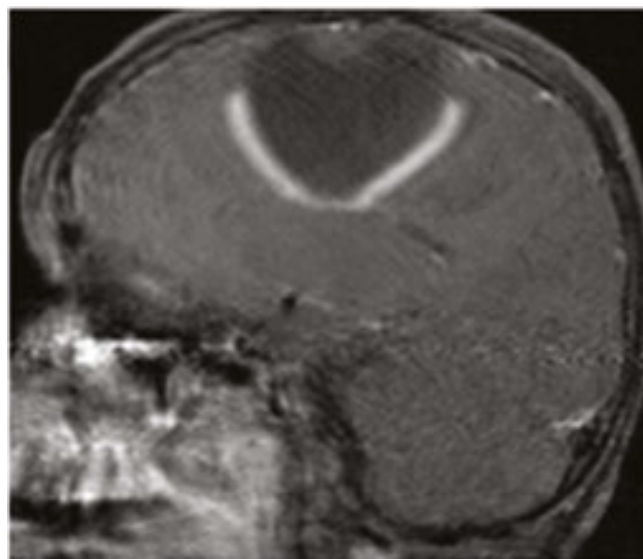

Figure 6. A case of TDL demonstarting incomplete rim enhancement on sagittal T1-weighted images after intravenous contrast administration.

5.1.1 Diffusion-weighted imaging

Min ADC values were higher in TDL than in PCNSLs or high-grade gliomas given that TDL is lesser cellular lesions than both PCNSLs and high-grade gliomas [18]. An important exception might be an acute demyelinating lesion which has areas of low ADC values (**Figure 7**). In acute phase in the TDL rim, there is peripheral restricted diffusion. The abnormal

diffusion resolves within 1–3 weeks. Following restricted diffusion on initial MRI, subsequent Gd enhancement can be seen [19].
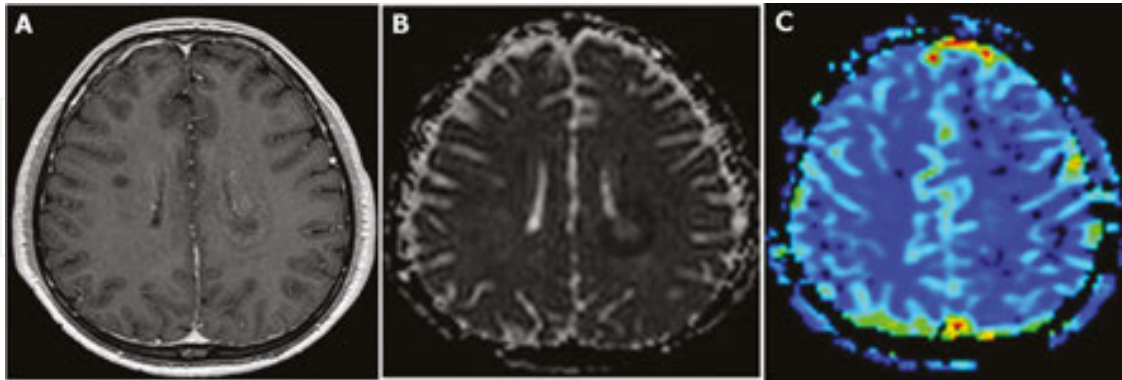

Figure 7. A case of TDL (A) demonstrating moderate ADC values (B). The rCBV maps show no elevation of Blood volume compared with contralateral normal white matter (C).

5.1.2. Perfusion imaging

TDL shows significant lower rCBV values (mean 0.88 ± 0.46) than high-grade gliomas (mean 6.47 ± 6.52), given the increased angiogenesis that the latter have (**Figure 7**). However, PCNSL had a less pronounced difference with a mean value of 2.11 ± 0.53 [20].

5.1.3. MR spectroscopy

TDL findings on spectroscopy are usually involve an elevated choline peak and reduced NAA signal. There may be also increased lactate and increased Cho/NAA that can reach high levels similar to that of high-grade gliomas; thus, differential diagnosis is problematic. The detection of glutamate and glutamine elevations has also been suggestive of TDL [21].

5.2. Brain abscess

Brain abscesses usually result from the extension of inflammation from the sinuses, the orbit, the mastoid cells, or the middle ear. As possible ways of spreading are either direct infection from a penetrating trauma, septic emboli, and contiguous or hematogenous spread. The most common pathogen is *Streptococcus pneumoniae*. Symptomatology is similar to any other mass lesions but tend to progress rapidly. Classical MRI findings of abscess in T2-weighted images are high-signal intensity with a thin rim of low intensity surrounded by edema. Furthermore, satellite lesions are more common in abscesses contrary to neoplastic lesions.

5.2.1. Diffusion-weighted imaging

The characteristic finding of brain abscess in DWI is a core of restricted diffusion due to pus consistency, whereas in neoplasms, there is usually low DWI signal (**Figure 8**). However, some necrotic brain metastasis may also display high signal intensity on DWI [22]. ADC values

usually increase as treatment is successful even if cavity remains. Another finding in the rim of neoplastic lesions is a lower ADC value than that of an abscess.
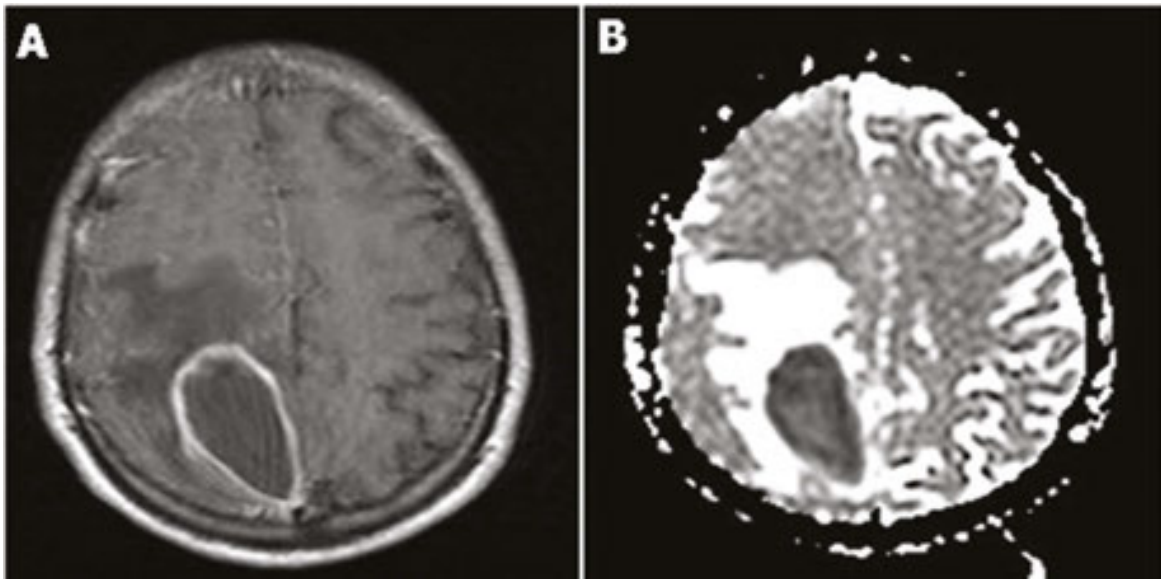

Figure 8. A case of an abscess (A) revealing low ADC values corresponding to the nonenhancing portion of the abscess (B).

5.2.2. Perfusion imaging

Contrary to glioblastomas and metastases, the enhancing rims of abscesses usually demonstrate lower rCBV values. The rCBV ratio of the enhancing portions of abscesses has be reported to be 0.79 ± 0.18, whereas in tumors was 1.40 ± 0.54 [23].

5.2.3. MR spectroscopy

Relative-specific MR spectroscopic feature of brain abscess is a succinate peak; however, it is not present in all cases. Apart from that elevated peaks of lactate, acetate, amino acids, alanine, valine, leucine, and isoleucine can be found. In abscesses reduced peaks of Cho/Crn and NAA are usually present [24]. Tuberculous abscesses typically have high lipid (mostly short-chain fatty acids such as butyric, isobutyric, caproic). Disappearance of metabolites of bacterial origin has been correlated with positive response to therapy [25].

5.3. Encephalitis

Encephalitis is an acute, usually diffuse, inflammatory process affecting the brain and may mimic mass lesions. Herpes simplex (HSV) encephalitis is the most common cause. Biopsy is helpful in some instances. Patients are usually confused and disoriented at the beginning and progress to coma within days. MRI demonstrates edema as high signal on T2, primarily within the temporal lobe, that may extend across sylvian fissure. Enhancement is usually present after the second week. Foci of hemorrhage occasionally can be found on MRI.

5.3.1. Diffusion-weighted imaging

Encephalitis typically demonstrates low ADC values due to cytotoxic edema. However, encephalitis may mimic an infarct that involves the cortical regions of the temporal lobe.

5.3.2. Perfusion imaging

Perfusion MRI has not been widely studied in encephalitis. At an early stage, there is an abnormal increase of blood flow in the affected area, followed by hypoperfusion at a later stage.

5.3.3. MR spectroscopy

On MR spectroscopy, finding encephalitis needs to be differentiated from a low-grade glioma which has similar findings. In general, there is a decrease in NAA peak usually 1–2 weeks after onset. After clinical recovery, there is a corresponding increase in NAA [26, 27]. Frequently, there is an increase in choline and myoinositol peak. An increased Cho/Cr ratio may be attributed to myelin breakdown. Sporadically, the lactate peak may be elevated.

5.4. Metastasis

Although the annual incidence of brain tumors is 17,000, for brain metastasis is 170,000 [28]. Thus, brain metastasis is the most common brain tumor seen clinically. The source of more than 50% of metastatic lesions is lung and breast cancer. When a single-brain lesion is found in a patient with a history of cancer, in 11% of these cases the lesion will not be metastatic. Four out of five of solitary metastases are located in the cerebral hemispheres. The majority tends to occur at the gray/white matter junction and is usually located posterior to the Sylvian fissure.

5.4.1. Diffusion-weighted imaging

The characteristic diffusion-weighted imaging feature for metastatic neoplasms is an elevated ADC. However, there is an overlap of the ADC values of metastatic lesions with those of primary neoplasms (**Figure 9**). Evaluation of ADC values in the non-enhancing T2-hyperintense areas surrounding the lesion may provide clues for the differentiation of high-grade gliomas from metastasis, given the lower ADC values in infiltrated areas of primary neoplasms compared with metastatic lesions. A threshold value of 1.302×10^{-3} mm^2/s for the minimum ADC value in the peritumoral regions had a sensitivity of 82.9% and specificity of 78.9% for distinguishing between glioblastoma and metastasis [29]. Although some studies have not found correlation between restricted diffusion or ADC values and various histologic types of metastases; however, a study reported that well-differentiated adenocarcinomas had lower DWI signal intensity compared with poorly differentiated carcinomas [30, 31].
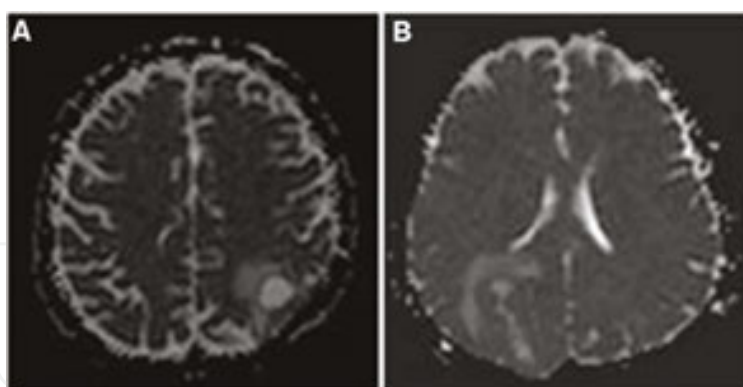
Figure 9. There is overlapping in the ADC values between a metastatic (A) and a primary brain tumor (B).

5.4.2. Perfusion imaging

Angiogenesis is essential for metastatic tumors growth. Thus, these lesions are associated with increased rCBV values compared with contralateral normal white matter. Thus, perfusion metrics tend to overlap between high-grade gliomas and metastatic lesions (**Figure 10**). The peak height and the percentage of signal intensity recovery derived from the T2* relaxivity curve on DSC MR has been reported to provide important clues [32]. Apart from that, metastasis from melanoma and renal cell carcinoma has been reported to have significant higher rCBV values than high-grade gliomas and metastases from lung cancer [33].
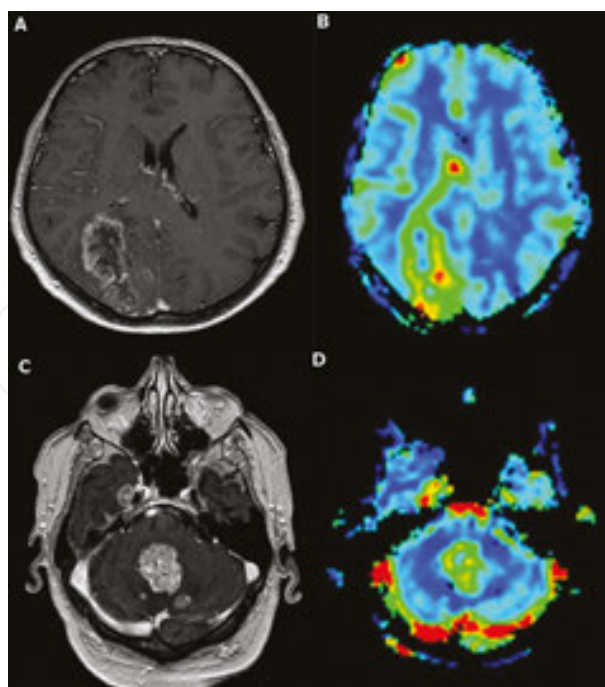

Figure 10. Both glioblastoma (A, B) and metastatic lesions (C, D) exhibits increased rCBV values, not permitting a differentiation based on perfusion imaging.

The rCBV values of perilesional area are usually higher for gliomas than metastatic lesions, due to glioma's infiltrative nature. In a study of 22 high-grade gliomas and 26 metastatic lesions, the rCBV ratios of peritumoural edema were 0.89 ± 0.51 in high-grade gliomas and 0.31 ± 0.12 in metastasis. A threshold rCBV value of 0.46 has been proposed, with a sensitivity of 77.3% and specificity of 96.2% for the differentiation of the two entities [34].

5.4.3. MR spectroscopy

Accurate differentiation between high-grade gliomas and metastatic lesion based on the enhancing part is problematic based on MR spectra. In metastatic lesions, there is no NAA peak, whereas necrosis results in a lipid peak. Lipid and lactate may be also elevated in primary brain tumors due to necrosis. Myoinosital peaks have not been reported to date in brain metastases, contrary to high-grade gliomas which tend to have elevated peaks [35, 36]. Given that primary tumors have a tendency to infiltrate, evaluation of the T2 hyperintense perilesional tissue provide more important information. Thus, although there is an intratumoral choline peak in both primary and metastatic lesions, there is no choline elevation in the peritumoural edema in metastatic lesions [37].

6. Conclusion

Intra-axial brain lesions are a significant health problem and are often a diagnostic imaging challenge. Advanced MRI techniques including proton spectroscopy, perfusion, and DWI have all been evaluated primarily in the context of distinguishing high-grade gliomas from metastases, abscess, and CNS lymphoma. Knowledge of the imaging characteristics of the most common intra-axial masses may allow the non-invasive diagnosis and classification of these masses.

Author details

Anastasia Zikou[1], George Alexiou[2*] and Maria Argyropoulou[1]

*Address all correspondence to: alexiougrg@yahoo.gr

1 Department of Radiology, School of Medicine, University of Ioannina, Ioannina, Greece

2 Department of Neurosurgery, School of Medicine, University of Ioannina, Ioannina, Greece

References

[1]   Ostrom QT, Gittleman H, Fulop J, Liu M, Blanda R, Kromer C, Wolinsky Y, Kruchko C, Barnholtz-Sloan JS. CBTRUS statistical report: primary brain and central nervous system tumors diagnosed in the United States in 2008–2012. Neuro Oncol. 2015;14(Suppl 4):iv1–62.

[2]   Alexiou GA, Zikou A, Tsiouris S, Goussia A, Kosta P, Papadopoulos A, Voulgaris S, Kyritsis AP, Fotopoulos AD, Argyropoulou MI. Correlation of diffusion tensor, dynamic susceptibility contrast MRI and (99m)Tc-Tetrofosmin brain SPECT with tumour grade and Ki-67 immunohistochemistry in glioma. Clin Neurol Neurosurg. 2014;116:41–5.

[3]   Würdinger T, Tannous BA. Glioma angiogenesis: towards novel RNA therapeutics. Cell Adh Migr. 2009;3(2):230–5.

[4]   Das S, Marsden PA. Angiogenesis in glioblastoma. N Engl J Med. 2013;369(16):1561–3.

[5]   Zikou AK, Alexiou GA, Kosta P, Goussia A, Astrakas L, Tsekeris P, Voulgaris S, Malamou-Mitsi V, Kyritsis AP, Argyropoulou MI. Diffusion tensor and dynamic susceptibility contrast MRI in glioblastoma. Clin Neurol Neurosurg. 2012;114(6):607–12.

[6]   Zikou A, Alexiou GA, Vartholomatos G, Goussia A, Xydis VG, Kosta P, Voulgaris S, Kyritsis AP, Argyropoulou MI. Correlation of diffusion tensor and dynamic susceptibility contrast MRI with DNA ploidy and cell cycle analysis of gliomas. Clin Neurol Neurosurg. 2015;139:119–24.

[7]   Cha S, Tihan T, Crawford F, Fischbein NJ, Chang S, Bollen A, Nelson SJ, Prados M, Berger MS, Dillon WP. Differentiation of low-grade oligodendrogliomas from low-grade astrocytomas by using quantitative blood-volume measurements derived from dynamic susceptibility contrast-enhanced MR imaging. AJNR Am J Neuroradiol. 2005;26(2):266–73.

[8]   Alexiou GA, Moschovi M, Stefanaki K, Sfakianos G, Prodromou N. Epidemiology of pediatric brain tumors in Greece (1991–2008). Experience from the Agia Sofia Children's Hospital. Cent Eur Neurosurg. 2011;72(1):1–4.

[9]   Wang Q, Zhang H, Zhang J, Wu C, Zhu W, Li F, Chen X, Xu B. The diagnostic performance of magnetic resonance spectroscopy in differentiating high-from low-grade gliomas: a systematic review and meta-analysis. Eur Radiol. 2015 Oct 15 [Epub ahead of print].

[10] Chen S, Tanaka S, Giannini C, et al. Gliomatosis cerebri: clinical characteristics, management, and outcomes. J Neurooncol. 2013;112(2):267–75.

[11] Fuller GN, Scheithauer BW. The 2007 revised World Health Organization (WHO) classification of tumors of the central nervous system: newly codified entities. Brain Pathol. 2007;17:304–7.

[12] Chen S, Tanaka S, Giannini C et-al. Gliomatosis cerebri: clinical characteristics, management, and outcomes. J Neurooncol. 2013;112(2):267–75.

[13] Desclée P, Rommel D, Hernalsteen D, Godfraind C, de Coene B, Cosnard G. Glioma-tosis cerebri, imaging findings of 12 cases. J Neuroradiol. 2010;37(3):148–58.

[14] Bendszus M, Warmuth-metz M, Klein R et-al. MR spectroscopy in gliomatosis cerebri. AJNR Am J Neuroradiol. 2000;21(2):375–80.

[15] Al-Okaili RN, Krejza J, Wang S, Woo JH, Melhem ER. Advanced MR imaging techni-ques in the diagnosis of intraaxial brain tumors in adults. Radiographics. 2006;26(Suppl 1):S173–89.

[16] Hartmann M, Heiland S, Harting I, Tronnier VM, Sommer C, Ludwig R, Sartor K. Distinguishing of primary cerebral lymphoma from high-grade glioma with perfu-sion-weighted magnetic resonance imaging. Neurosci Lett. 2003;338(2):119–22.

[17] Yamasaki F, Takayasu T, Nosaka R, Amatya VJ, Doskaliyev A, Akiyama Y, Tomina-ga A, Takeshima Y, Sugiyama K, Kurisu K. Magnetic resonance spectroscopy detec-tion of high lipid levels in intraaxial tumors without central necrosis: a characteristic of malignant lymphoma. J Neurosurg. 2015;122(6):1370–9.

[18] Mabray MC, Cohen BA, Villanueva-Meyer JE, Valles FE, Barajas RF, Rubenstein JL, Cha S. Performance of apparent diffusion coefficient values and conventional MRI features in differentiating tumefactive demyelinating lesions from primary brain neoplasms. AJR Am J Roentgenol. 2015;205(5):1075–85.

[19] Hyland M, Bermel RA, Cohen JA. Restricted diffusion preceding gadolinium enhance-ment in large or tumefactive demyelinating lesions. Neurol Clin Pract. 2013;3(1):15–21.

[20] Cha S, Pierce S, Knopp EA, Johnson G, Yang C, Ton A, Litt AW, Zagzag D. Dynamic contrast-enhanced T2*-weighted MR imaging of tumefactive demyelinating lesions. AJNR Am J Neuroradiol. 2001;22(6):1109–16.

[21] Al-Okaili RN, Krejza J, Wang S, Woo JH, Melhem ER. Advanced MR imaging techni-ques in the diagnosis of intraaxial brain tumors in adults. Radiographics. 2006;26(Suppl 1):S173–89.

[22] Park SH, Chang KH, Song IC, Kim YJ, Kim SH, Han MH. Diffusion-weighted MRI in cystic or necrotic intracranial lesions. Neuroradiology. 2000;42:716–21.

[23] Holmes TM, Petrella JR, Provenzale JM. Distinction between cerebral abscesses and high-grade neoplasms by dynamic susceptibility contrast perfusion MRI. AJR Am J Roentgenol. 2004;183(5):1247–52.

[24] Pal D, Bhattacharyya A, Husain M, Prasad KN, Pandey CM, Gupta RK. In vivo proton MR spectroscopy evaluation of pyogenic brain abscesses: a report of 194 cases. AJNR Am J Neuroradiol. 2010;31(2):360–6.

[25] Lai PH, Weng HH, Chen CY, Hsu SS, Ding S, Ko CW, Fu JH, Liang HL, Chen KH. In vivo differentiation of aerobic brain abscesses and necrotic glioblastomas multiforme using proton MR spectroscopic imaging. AJNR Am J Neuroradiol. 2008;29(8):1511–8.

[26] Sämann PG, Schlegel J, Müller G, Prantl F, Emminger C, Auer DP. Serial proton MR spectroscopy and diffusion imaging findings in HIV-related herpes simplex encephalitis. AJNR Am J Neuroradiol. 2003;24(10):2015–9.

[27] Takanashi J, Sugita K, Ishii M, Aoyagi M, Niimi H. Longitudinal MR imaging and proton MR spectroscopy in herpes simplex encephalitis. J Neurol Sci. 1997;149(1):99–102.

[28] Johnson J D, Young B. Demographics of brain metastasis. Neurosurg Clin N Am. 1996;7(3):337–44.

[29] Lee EJ, terBrugge K, Mikulis D, Choi DS, Bae JM, Lee SK, Moon SY. Diagnostic value of peritumoral minimum apparent diffusion coefficient for differentiation of glioblastoma multiforme from solitary metastatic lesions. AJR Am J Roentgenol. 2011;196(1): 71–6.

[30] Hayashida Y, Hirai T, Morishita S, Kitajima M, Murakami R, Korogi Y, et al. Diffusion-weighted imaging of metastatic brain tumors: comparison with histologic type and tumor cellularity. AJNR Am J Neuroradiol. 2006;27:1419–25.

[31] Duygulu G, Ovali GY, Calli C, Kitis O, Yünten N, Akalin T, et al. Intracerebral metastasis showing restricted diffusion: correlation with histopathologic findings. Eur J Radiol. 2010;74:117–20.

[32] Cha S, Lupo JM, Chen MH, Lamborn KR, McDermott MW, Berger MS, Nelson SJ, Dillon WP. Differentiation of glioblastoma multiforme and single brain metastasis by peak height and percentage of signal intensity recovery derived from dynamic susceptibility-weighted contrast-enhanced perfusion MR imaging. AJNR Am J Neuroradiol. 2007;28(6):1078–84.

[33] Kremer S, Grand S, Berger F, Hoffmann D, Pasquier B, Rémy C, Benabid AL, Bas JF. Dynamic contrast-enhanced MRI: differentiating melanoma and renal carcinoma metastases from high-grade astrocytomas and other metastases. Neuroradiology. 2003;45(1):44–9.

[34] Hakyemez B, Erdogan C, Gokalp G, Dusak A, Parlak M. Solitary metastases and high-grade gliomas: radiological differentiation by morphometric analysis and perfusion-weighted MRI. Clin Radiol. 2010;65(1):15–20.

[35] Bendini M, Marton E, Feletti A, Rossi S, Curtolo S, Inches I, et al. Primary and metastatic intraaxial brain tumors: prospective comparison of multivoxel 2D chemical-shift

imaging (CSI) proton MR spectroscopy, perfusion MRI, and histopathological find-
ings in a group of 159 patients. Acta Neurochir (Wien). 2011;153:403–12.

[36] Fan G, Sun B, Wu Z, Guo Q, Guo Y. In vivo single-voxel proton MR spectroscopy in
the differentiation of high-grade gliomas and solitary metastases. Clin Radiol.
2004;59:77–85.

[37] Fink KR, Fink JR. Imaging of brain metastases. Surg Neurol Int. 2013;4(Suppl 4):S209–
19.